

New Experimental Device to Test the Dynamic Behavior of Fiber Assemblies and Fibrous Composite Structures with a Focus on Larger Industrial-Scale-Like Samples

S. Rebouillat,¹ D. Liksonov,² A. Courgey³

¹DuPont Int. Op. Sarl, DPT-AFS, CH1218, Le Grand Saconnex, Geneva, Switzerland

²ISAT-ENSMM-ISPU, Mech. Eng. Dept., 38 rue Battant 25000 Besançon, France

³Magnitude Research Center, Mech. Eng. Dept., 58470 Magny-Cours, France

Received 3 January 2011; accepted 5 April 2011

DOI 10.1002/app.34626

Published online 19 August 2011 in Wiley Online Library (wileyonlinelibrary.com).

ABSTRACT: This article focuses on the development of an experimental measurement system intended for dynamic mechanical analysis (DMA) of fiber structures. First, a short review of DMA testing procedures is given, followed by an analysis of particularities of DMA application to fibers and rope assemblies. The necessity of developing a dedicated device for fiber assembly and rope applications is pointed out, as the commercial DMA testing devices available are intended for shorter specimens. Thus, the article insists on the underlying necessity to come up with a measurement device for much longer fiber specimens and a testing procedure therewith. Then the article presents the main concepts of the new device and its operation. Three different operating modes are

presented with explanations of their functioning, their particularities, and the interest for rope testing. After that, the implementation of the testing device prototype is presented, describing the mechanical set up, electromagnetic elements, power and acquisition circuitry and software. At last, preliminary experimental results are provided demonstrating the feasibility of this solution and indications concerning the potential future developments of this kind of rope testing systems are given. © 2011 Wiley Periodicals, Inc. *J Appl Polym Sci* 123: 1708–1717, 2012

Key words: dynamic mechanical analysis; fibers; filaments; cords; resonance; damping; viscoelasticity; storage modulus; loss tangent; dissipation factor; fatigue; composite structures

INTRODUCTION

Dynamic mechanical analysis (DMA) and dynamic mechanical thermal analysis (DMTA) are the methods used to characterize the stiffness and damping properties of a material.¹ In DMA, the sample is most often deformed and released by applying a sinusoidal load. Modulus is calculated from the amplitudes of motion and force, while damping is measured from the time delay (phase lag) between the applied force and the resulting motion.² Damping is expressed in terms of $\tan \delta$ and is related to the amount of energy a material can store.¹ Stiffness and damping properties are often studied as a function of frequency, applied force, temperature, or other parameters. Other properties, such as storage modulus, loss modulus, viscosities, compliance, etc., can be derived from these measurements. According to Ref. ¹, DMA is the most sensitive technique for

monitoring relaxation events, such as glass transitions, as the mechanical properties change dramatically when relaxation behavior is observed. Most DMA analyzers are also capable of operating in the creep–recovery mode.³

Rebouillat et al.^{4–10} have made and reported considerable amount of work to characterize fiber surface treatments as well as joint adhesion structural strength and ageing performance. Combined with other analytical tools, the DMA and DMTA are able to compete with differential scanning calorimetry, combined or not with thermo gravimetric analysis to identify polymeric transitions and to a certain extend subtransitions. As underlined in Refs. ^{11,12}, especially suitable applications are associated with the use of aramids and carbon fibers, especially aramid fibers, which most of the time are used as reinforcing elements therefore impregnated, such as in aeronautic, aerospace, marine, automotive, military, and civil protection end-uses.

More recently, Rebouillat and Liksonov¹³ made a review of the modeling of liquid–solid interactions in partially filled containers used under rather extreme conditions in for example racing vehicles, space shuttles, etc. DMA analysis is also a very

Correspondence to: S. Rebouillat (serge.rebouillat@che.dupont.com).

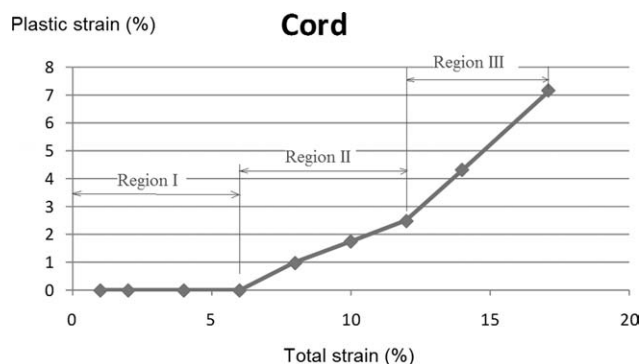


Figure 1 Nylon cord: three different behavior zones during a tensile test (after putting it under stress). I: Pure elastic; II: Elastoplastic with elastic prevailing; fiber deformation in the crossings zones; III: Elastoplastic with plastic prevailing; fiber deformation over the total length; elongation.

useful tool to measure the damping behavior of the wall structures under resonance conditions in some cases.³

Apart from more traditional applications of DMA in studying bulk viscoelastic materials, some researchers^{14–20} have recently turned their attention to applications involving the viscoelasticity of fibers, cords, and filaments. The results obtained by Refs. ^{14,16}, as well as the theoretical developments by these authors, indicate that the DMA data, being closely related to loss due to fiber-on-fiber friction, provides a new approach and opportunity for fiber-on-fiber friction research. The energy dissipated due to fiber-on-fiber friction is a direct reflection of the friction phenomenon, and therefore, the authors¹⁴ propose to use the energy dissipation to characterize fiber-on-fiber friction. This should create a wide new range of applications for DMA testing of ropes, cords, and yarns, with the final goal of studying or improving their friction and wear properties.

However, most commercially available DMA testing machines are not well adapted for filament testing. The following limitations are the most common:

- Size of the specimen (length) is often limited (typically to 3–6 cm), as great length is not required for bulk specimens. However, this is a very important issue for cords, as the sample length should be much longer than one complete turn (twist) length.¹⁴ In fact, for example a gage length significantly shorter than the staple length results in a considerably lower energy loss due to lack of relative movement of the fibers.¹⁴ Besides that, high dispersion was observed during experiments with short (around 3 cm) samples.

- Maximum tensile displacement allowed by DMA testing devices may be insufficient for long filament or cord samples.
- The method used in the commercial equipment (forced sine oscillations) is not perfectly adapted to measure very low $\tan \delta$ values that we observed in our experiments (see Fig. 3). Under these conditions, free vibration based techniques may be expected to provide better results.

Especially critical material to test are the structures and cord assemblies which comprise a fairly large number of substructures such as subcord-assemblies made of yarns, the later made of filaments, sometimes only a few microns in diameter.¹¹

Figures 1 and 2 show the behavior of a nylon cord (5000 dtex, about 1 mm diameter) and of a nylon filament (300 μm diameter) under a traditional stress/strain static analysis. The cord structure shows three distinct regions, while the filament exhibits a progressive creeping behavior. The DMA and DMTA are able to distinguish those regions, unfortunately the variation using a commercial DMA are large as shown in Figure 3, especially in the conditioning preload case of 80 N. This lack of reproducibility and repeatability is inherent to the size of the sample, a few centimeters (2–3 cm) and the operating difficulties associated with the handling of such samples made of a large number of filaments.

Due to the above considerations, and after having accomplished multiple tests of fibers samples on a commercial DMA machine, it has been decided to develop a dedicated testing device for fiber assemblies to overcome the existing DMA equipment limitations. The efforts were in particular focused on measuring the DMA parameters of higher length specimens with weak $\tan \delta$. Another important objective was fatigue testing that also finds numerous applications in fiber assemblies and structures^{21,22}: performing large number of cycles at a sufficiently high frequency and at affordable cost of investment,

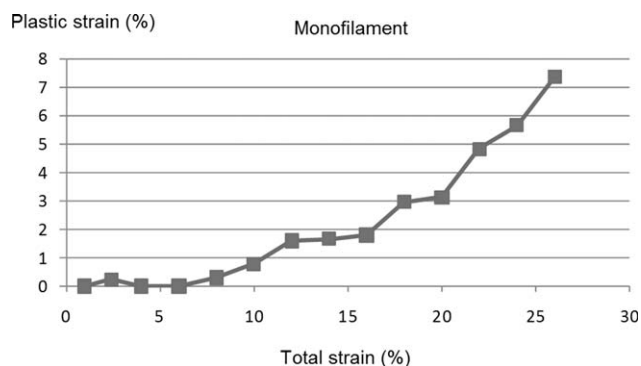


Figure 2 Nylon filament: gradual transition from elastic to plastic behavior.

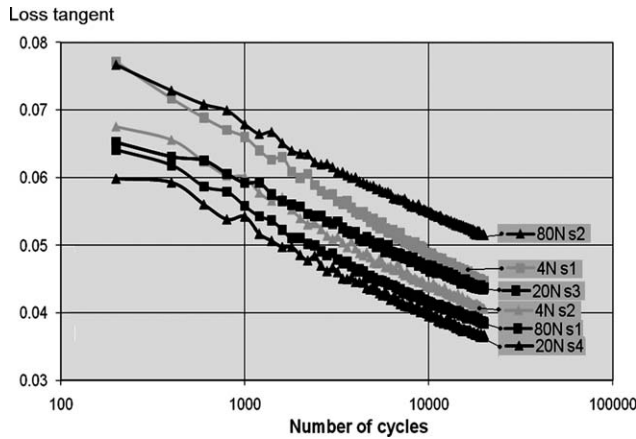


Figure 3 Continuous drop of damping and lack of reproducibility. Prestressed cord samples with prestress values of 4, 20, and 80 N (2 sample repeats per conditioning preload). Loss tangent evolution as a function of the number of cycles (Fstat 45 N, Fdyn ±15 N).

maintenance, and operation. Frictionless design has been employed to reduce the wear of key elements.

MATERIALS AND METHODS

Materials

The following components and pieces of equipment have been used to make up the testing system:

- Laptop PC for control, signal processing, and visualization purposes.
- Multichannel signal acquisition board (USB connection to the PC).
- Function waveform generator.

- Various electrical and electronic components for control and acquisition circuitry.
- Strong neodymium–iron–boron (NdFeB) magnets for an actuator.
- Aluminum profile for a rigid mechanical set up.
- Auxiliary workshop consumables.

Method of DMA operation and operating modes

The basic principle of system operation consists in applying a dynamic force load to prestrained (under static load assured by a weight) cord segments (upper and lower, symmetric) and registering the cord displacements. This force load is applied by means of an actuator consisting of two coils and several ring NdFeB magnets. The displacement is measured using Hall sensors and a linear variable differential transformer (LVDT), and its displacement velocity using symmetrical coils around a magnet. A more detailed explanation is provided in the “Test equipment operation methods and signal processing” section and in Figures 6–8.

Three operating modes have been implemented: pulse mode, sine mode, and resonance mode.³

The pulse mode (Fig. 4) is characterized by free oscillations of the “spring–mass” resonance system made up by the actuator rod and two cord segments. In the pulse mode, this system is put into motion by a pulse of current in the actuator coils. The material properties are then determined as follows, based on vibration theory and general mechanics equations:²³

System stiffness: $K_{sys} = m (2 \cdot \pi \cdot f)^2$, where m —vibrating mass, f —free oscillation frequency.

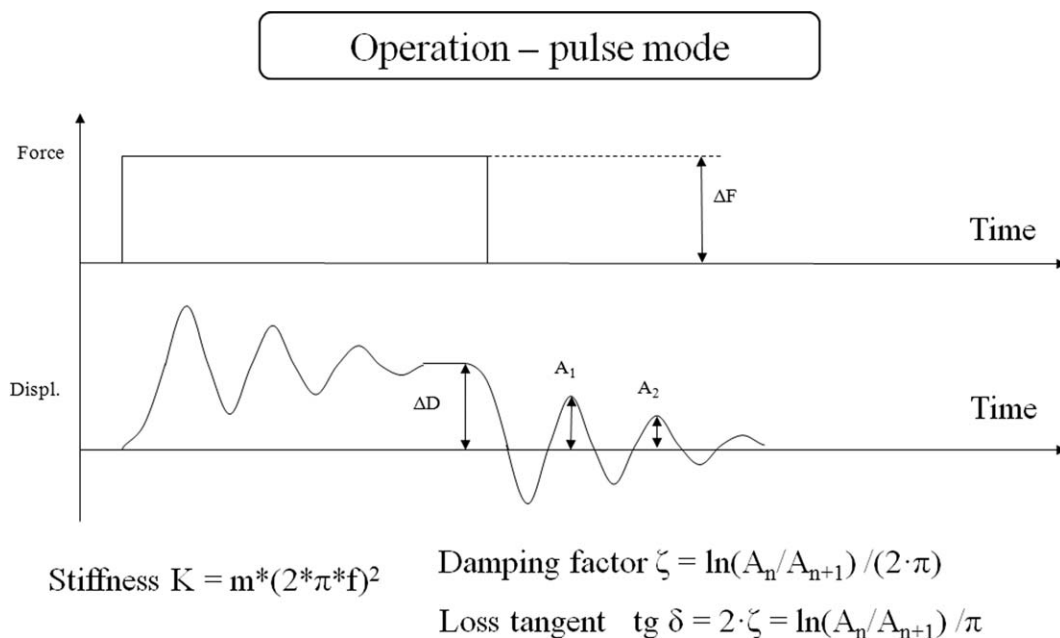


Figure 4 Pulse mode DMA operation.

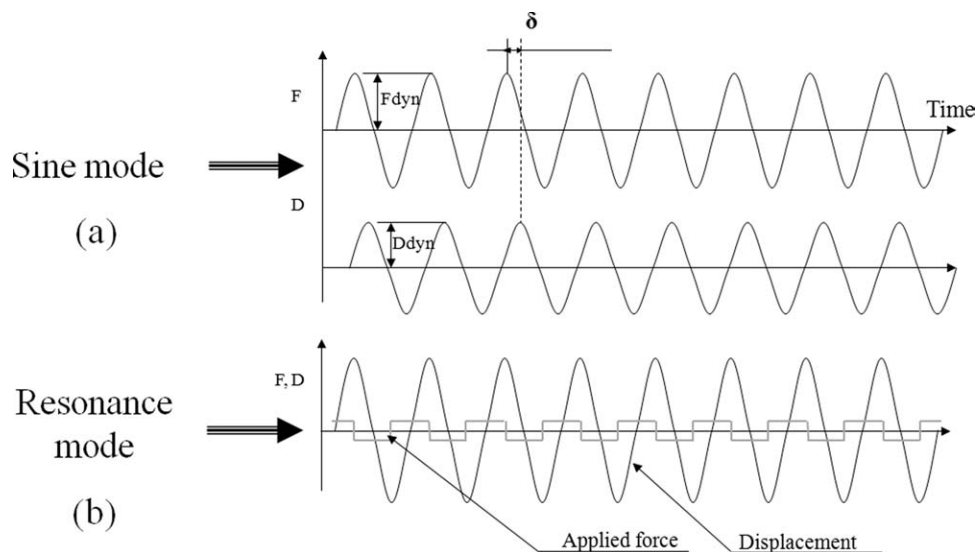


Figure 5 Sine mode (a) and resonance mode (b) DMA operation.

Stiffness of the cord (per length unit): $K_{\text{cord}} = K_{\text{sys}} \cdot L_{\text{top}} \cdot L_{\text{bot}} / (L_{\text{top}} + L_{\text{bot}})$, where L_{top} —free length of the top cord segment, L_{bot} —free length of the bottom cord segment.

Damping ratio (as defined in vibration theory): $\zeta = \ln(A_n/A_{n+1})/(2\pi)$, where A_{n-1} and A_n are the amplitudes of two successive oscillations.

$$\text{Loss tangent : } \text{tg } \delta = 2\zeta = \ln(A_n/A_{n+1})/\pi$$

The sine mode [Fig. 5(a)] is defined by forced sinusoidal motion of cord fragments under the dynamic load created by the actuator coils. It has been implemented primarily to assure comparability with the commercial DMA testing system. The stiffness and damping are determined directly from force/displacement amplitude ratio and phase lag in this mode³ as shown in Figure 5(a).

The resonance mode [Fig. 5(b)] is characterized by the motion of the actuator rod and cord segments at a frequency close to the free resonance frequency of this system. This motion is assured by the positive feedback from the velocity sensor that is used to control the direction of the electric current in the actuator coils. The principal application of this mode is fatigue testing of cord samples. Thanks to a relatively high operating frequency (typically 50–200 Hz) and to the frictionless design assuring the absence of frictional motion anywhere else than in the cord sample, a large number of cycles can be easily performed at reasonable costs.

The resonance mode can also be employed for cord sample DMA characterization at higher dynamic loads and to the study of cord properties evolution versus the number of cycles performed.

Test equipment operation methods and signal processing

The structural scheme of the testing device is shown in Figure 6. The power module controls the applied dynamic load by controlling the current in the actuator coils by means of a precision resistor and a feedback loop connected to an operational amplifier. The current and the dynamic load are proportional to the input (CURRENT CONTROL) voltage of the power module. The force value and shape of the force versus time curve can thus be easily controlled. The system can be driven either by a function generator or by a DAC card connected to a PC. In the pulse mode, rectangular pulses of low (0.2–3 Hz) frequency are employed and during the sine mode operation, sine waves of varying frequencies are used. These waveforms are created using a data acquisition board connected to a portable PC with the Labview[®] software.

The position can be measured by using either an LVDT or a combine position/velocity electromagnetic sensor. The conditioning and amplification of the sensor signals is assured by an acquisition module connected to an ADC card. The velocity signal is also used to create a positive feedback during the resonance mode operation; in this mode, the actuator current and force directions are switched to the opposite every time the velocity changes its sign.

The ADC card, controlled by the Labview[®] software, converts the sensor signals into the digital form at 2–10 kHz sampling rate and transmit them to a PC. The signals are then processed using a program in the C language that performs filtering,²⁴ interpolation, peak, and resonance frequency detection, and calculation of the output results (stiffness and damping factor estimations).

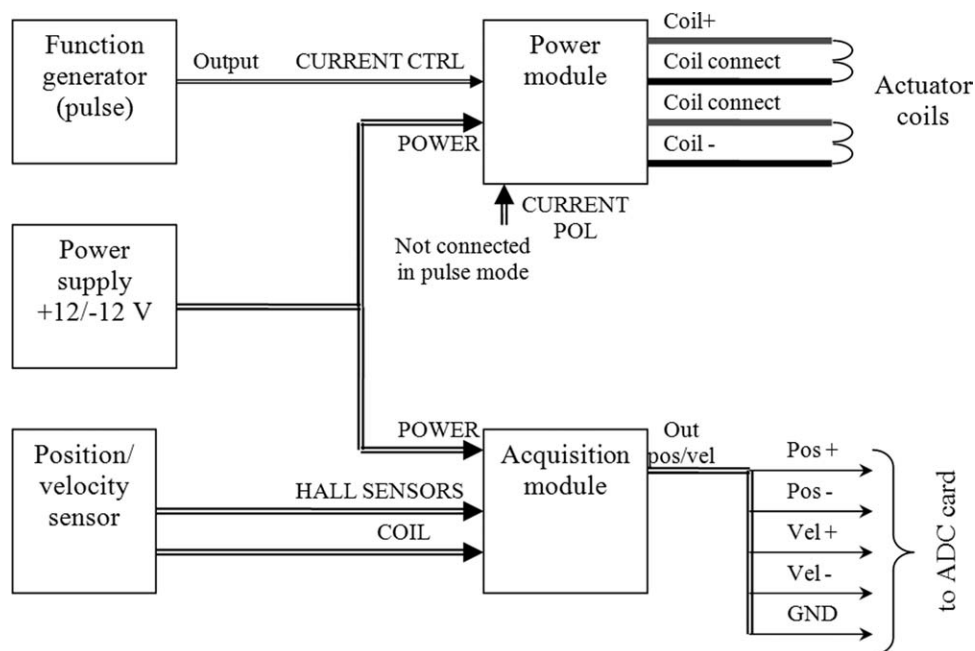


Figure 6 Structural scheme of the DMA cord testing system.

RESULTS AND DISCUSSION

Implementation of the testing system: Description of the mechanical set up, actuator and sensors

The mechanical structure of the measurement system is shown in Figures 7 and 8. The whole mechanical set up is mounted on a rigid vertical aluminum profile rail. The central moving element of the set up is a stainless steel rod with permanent ring NdFeB magnets mounted on it [Figs. 7(b) and 8(b)]. Two power coils each containing 150 turns of $\varnothing 0.5$ mm wire, attached to the base are placed near the set of two to four ring NdFeB magnets, thus making up the actuator.

Near the other end of the rod, at a sufficient distance from the actuator, another permanent magnet is fixed. Its magnetic field is measured by six Hall effect sensors (three on each side at 120° angles, see Fig. 9) allowing to determine its position, and the variations of the magnetic field induce voltages in the sensor coils, allowing to measure the velocity. Thus the six Hall sensors and two coils make up a combined displacement-velocity sensor. Alternatively, this sensor can be replaced by a custom-made LVDT (friction-free design), which is less sensible to lateral motion but does not allow to measure the velocity directly.

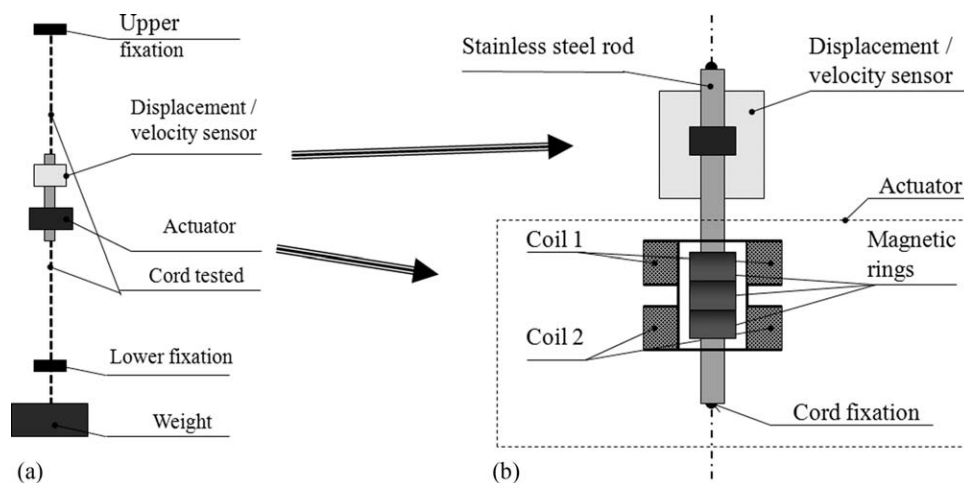


Figure 7 Mechanical structure of the DMA measurement system: (a) general structure; (b) central stainless steel rod with actuator, sensors, and permanent ring NdFeB magnets.

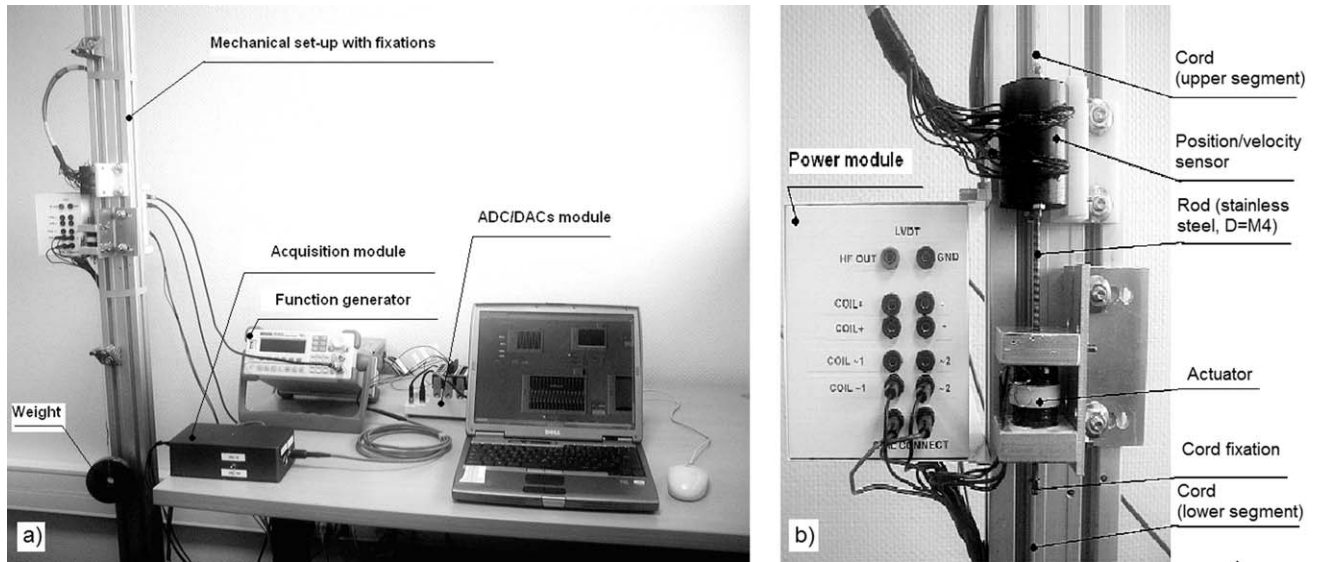


Figure 8 DMA measurement system prototype: (a) general view; (b) actuator/sensor block.

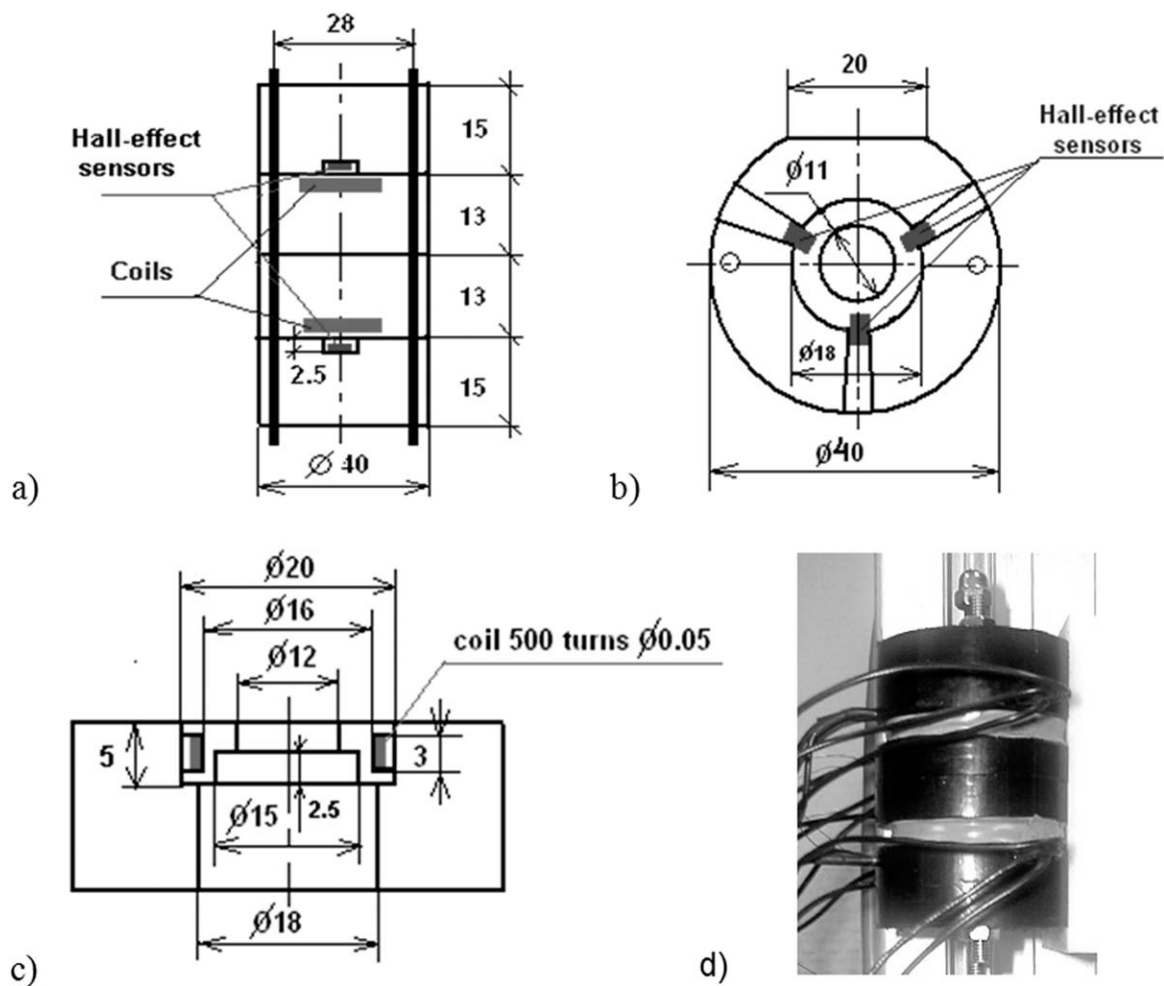


Figure 9 Combined velocity-position sensor: (a) frontal view; (b) Hall-effect sensor placement; (c) coil placement (section view); (d) photo of the combined sensor.

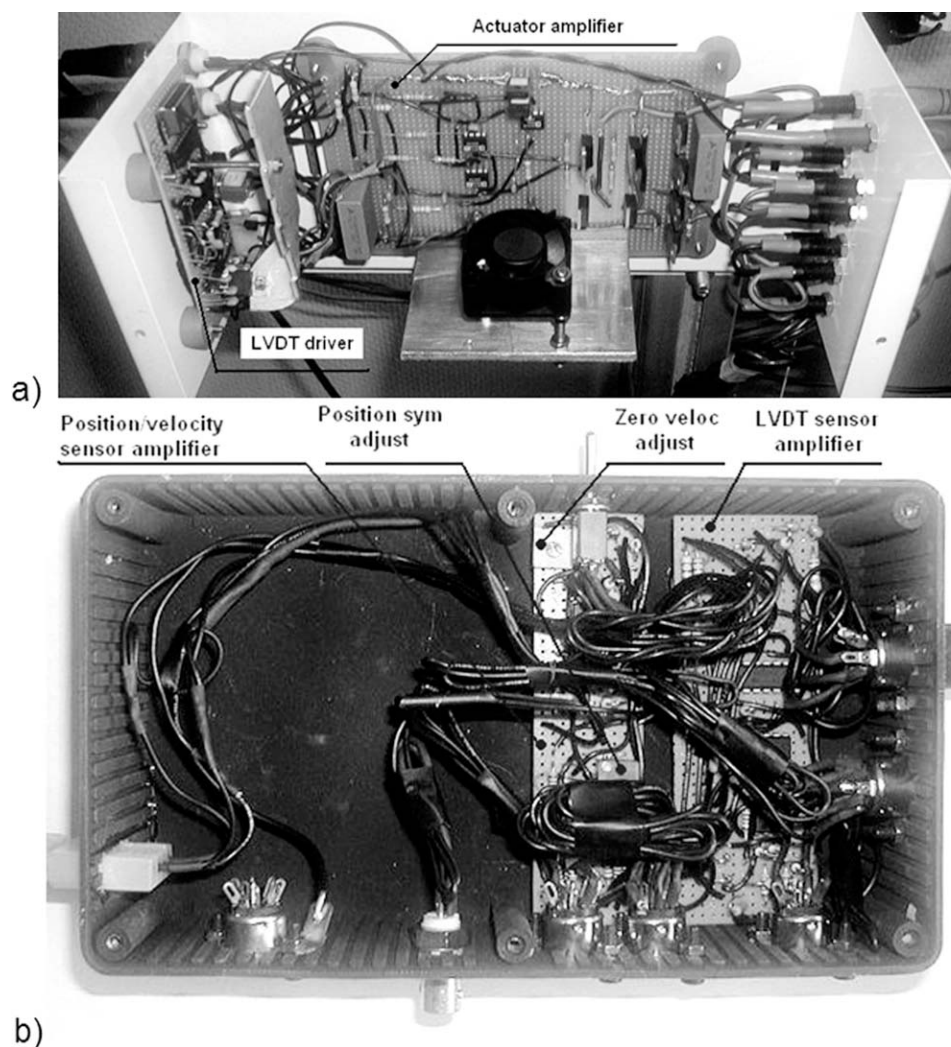


Figure 10 Electronic circuitry of the DMA cord testing system: (a) power module; (b) acquisition module.

Two cord samples are attached to the moving rod upper and lower extremities. The opposite end of each sample is fixed to the aluminum profile base. A static load is applied using a weight attached to the lower sample through a rod.

Implementation of the testing system: Electronic equipment and software

The electronic equipment ensuring the measurement system operation consists of two principal blocks (modules): power module [Fig. 10(a)] and acquisition module [Fig. 10(b)].

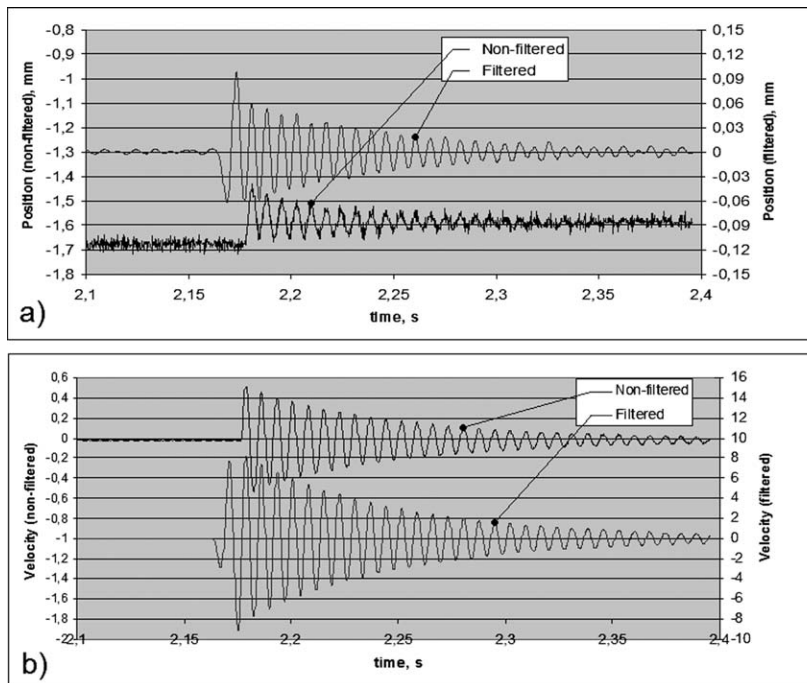
The power module controls the actuator coils and the LVDT sensor. Power MOSFETs have been used to deliver high current (up to 25 A) to the actuator coils. The current-regulation MOSFET is driven by an OPAMP using a feedback loop with a current-sensing precision resistor. Thus the system allows to deliver the current proportional to the input voltage. The same module contains also an LVDT driver

circuit that generates a stable signal (shape close to that of a sine wave) at 19.2 kHz frequency.

The acquisition module (Fig. 10) contains the circuits allowing to acquire the position and velocity signals. These circuits contain:

- Hall-effect position sensor preamplifier with zero (symmetry) adjustment.
- Velocity sensor preamplifier.
- LDVT sensor synchronous detector/conditioner with a switched-capacitor low-pass filter.
- Feedback comparator block for controlling the current direction in the resonance mode.

The conditioned/amplified sensor signals at the acquisition module outputs are sampled using an ADC card connected to a PC. The Labview[®] environment is used for basic system operation control and data acquisition. In addition to that, custom software that performs the signal processing and stiffness/damping results calculation in the pulse



Testing conditions:

- Cord:** white N3
- Fimp** = 2,2 N
- Fstat** = 12 N
- l** = 194 mm
- fs** = 5 kHz

Results (on filtered velocity signal):

- Loss tangent (averaged)** = 0.03268
- Stdev** = 0.000396

Figure 11 Typical acquired signal in the pulse mode: (a) position; (b) velocity signal.

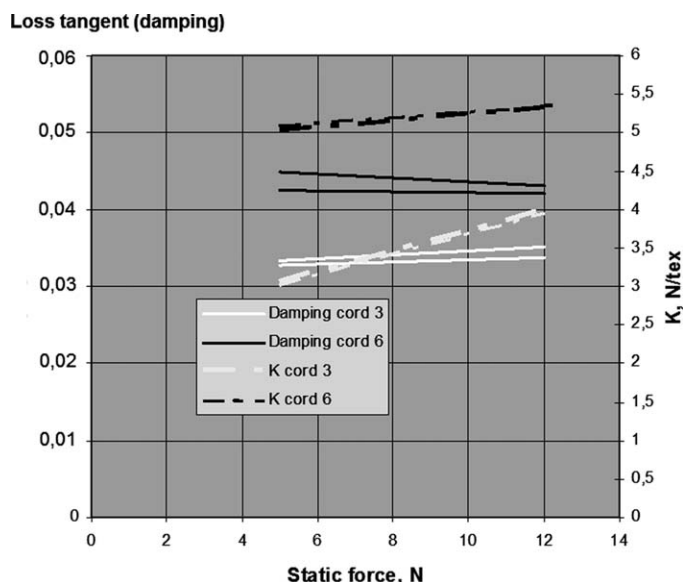
mode has been developed in the C language. In this software, the acquired velocity sensor signal is at first smoothed by a digital low-pass FIR filter²⁴ to reduce the HF noise level. Then, it is interpolated by a second-order polynomial near the local extremities (peak minimum and maximum values) for more accurate determination of peaking levels and times. Then, the nearby peaks are used to determine the resonance frequency and decay coefficient. Several subsequent measurements with averaging allow to calculate the final stiffness and damping results, based on the for-

mulae presented in the “Method of DMA operation and operating modes” section of this article.

Preliminary tests with their results. Comparison with a commercial DMA system

To validate the measurement system functioning and estimate the measurement precision, several preliminary tests have been performed.

The system has been tested in the pulse mode using two types of commercial polymeric cords: N#3 (not impregnated) and N#6 (impregnated). A static



Testing conditions:

- Fimp** = 1 N
- Fstat** = 5...12 N
- fs** = 5 kHz
- l** ≈ 210 mm
- Sensor** – velocity (coil)

Figure 12 DMA processing results: stiffness and damping as a function of static force for two types of cords with different impregnation (N#3 and N#6, 2 samples of each).

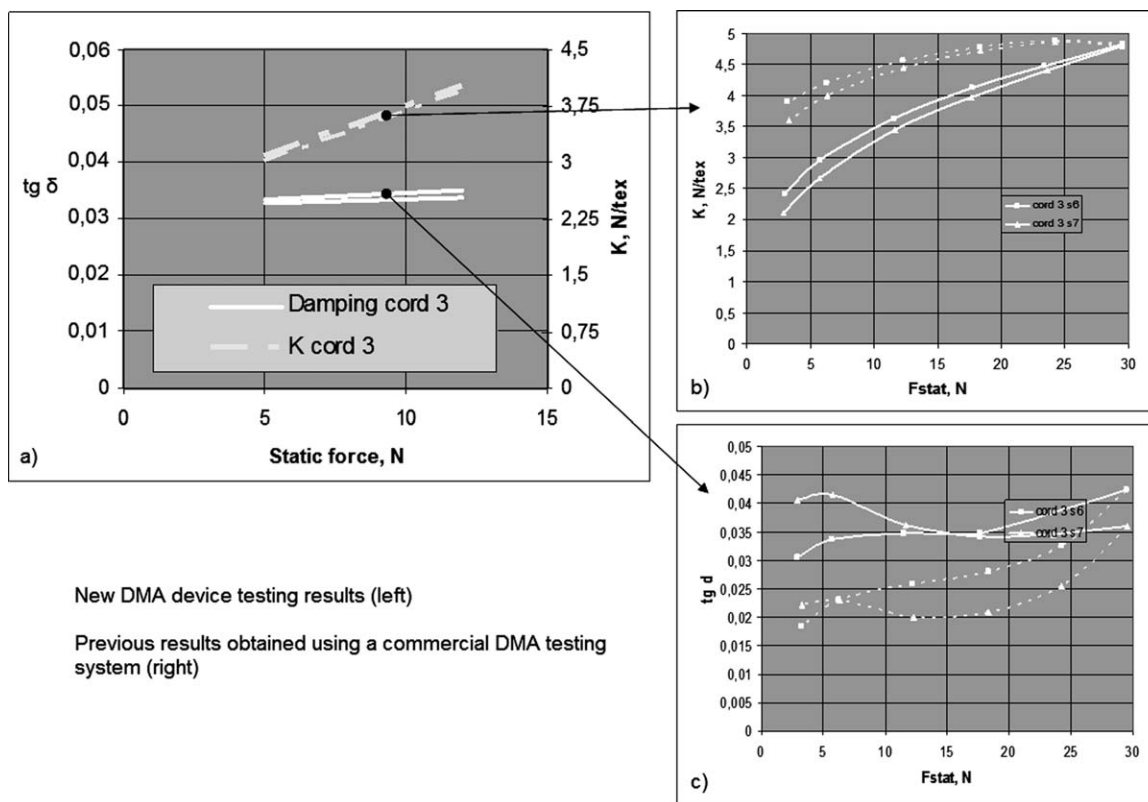


Figure 13 Comparative results for cord N#3: (a) New results obtained using the designed cord testing system; (b) Previous stiffness results obtained using a commercial DMA testing system; (c) Previous damping results on a commercial DMA system.

force varying in the 5–12 N range was applied, with pulses of 1 N amplitude. The cord samples used were ~ 20 cm length. The typical acquired signal is shown in Figure 11, and the processing results in Figure 12. They indicate relatively weak dispersion and good capacity of this method to distinguish between these two cord types.

The measurement results for cord N#3 have been also compared with those obtained using a commercial DMA system. Based on these results, we can conclude (Fig. 13), that:

- Dynamic stiffness results obtained using this new system are comparable with those obtained with much more expensive commercial equipment, despite different measurement methods employed.
- Damping factor results also seem to be comparable.
- There is less dispersion in the pulse mode on new device.
- New results seem to be little of not dependent from duration of testing and on exact procedure settings.

The differences observed in new results in comparison with commercial equipment can be explained by

the differences in the measurement method used (free oscillations following a pulse excitation in the new device vs. imposed sine wave in commercial equipment, as demonstrated in Figs. 4 and 5) and in the testing conditions.

Some preliminary tests have been also made in the sine wave mode, giving comparable results with commercial equipment. The system has also been successfully brought into oscillatory regime using the velocity signal feedback (resonance mode, see Fig. 14), thus demonstrating the feasibility of the resonance mode approach.

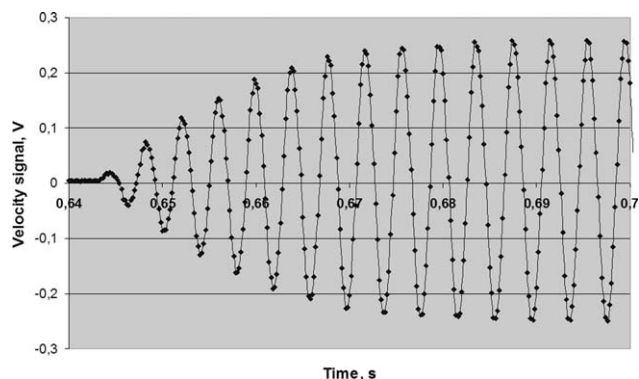


Figure 14 Demonstration of the velocity signal in the resonance mode.

It is worthwhile to stress the fact that the results are inline with commercial equipment's ones, as mentioned before at several occasions. In anticipation to reader's questions, it should also be underlined that this work is unique in terms of providing a larger scale sample testing device more suitable for industrial scientific research. This has never been achieved before; therefore, a more substantial data base needs to be established. The fact that the validation results are in line with known in the art data, does not remove the fact that those published data suffer tremendous reproducibility and repeatability issues due to the commercial equipment limitations with regard to the type of samples, which are tested within the scope of this work. The sample size, which commercial equipment can accommodate, is the major limitation. This is augmented by the appearance of defects, in industrially manufactured products, which are generally distributed along the samples in a way that does not allow a statistically proper detection and impact quantification when much smaller samples are used.

CONCLUSION

The dedicated measurement system developed for DMA and fatigue testing of cord segments has shown adequate results, with the measured stiffness and damping comparable with those obtained using a commercial measurement equipment. Thus, the feasibility of this approach has been demonstrated. The principal advantages of the system are the following:

- Operation in three different modes.
- Low component (several hundred euros) and maintenance cost.
- Completely open modular system can be modified and adapted to different applications.
- Results regarding the stiffness and the loss tangent compare well with standard DMA tests, as discussed in "Preliminary tests with their results. Comparison with a commercial DMA system" section.
- Adapted for longer cord samples (10–30 cm) in comparison with commercial equipment (up to 3–6 cm).
- The pulse mode is well adapted for weak loss factor measurement found in cord samples.
- Interesting potential for fatigues testing in the resonance mode (large number of cycles in short time, because of high frequency, typically 50–200 Hz; this frequency is higher than the typical frequencies in DMA analysis for our applications to cords/yarns, limited to 10–30 Hz because of resonance problems).

However, some effort might be required to adapt this prototype containing some manually made components (actuator, sensor blocks, etc.) for industrial implementation. Besides that, additional work is needed to fully implement the signal processing in the resonance mode.

Future research work is been dedicated to this new approach to long waited "larger scale" dynamic mechanical testing in general.

References

1. Triton-technology. What is Dynamic Mechanical Analysis, DMA? Available at: http://www.triton-technology.co.uk/pdf/TTINF_WhatIsDMA_220110.pdf. Accessed on January 2010.
2. Van-de-Velde, J. G.; Foreman, J.; Weddle, B. A New Instrument for Dynamic Mechanical Analysis With Controlled-Temperature Exposure to Fluids or Humidity, Automotive Composites Conference, September 2001, MSU Management Education Center 811, Troy MI, USA. Available at: http://www.speautomotive.com/SPEA_CD/SPEA2001/pdf/a/A2.pdf.
3. Menard, K.P. Dynamic Mechanical Analysis: A Practical Introduction; CRC Press LLC: Boca Raton, 1999.
4. Rebouillat, S.; Escoubes, M.; Gauthier, R.; Vigier, A. *Polymer* 1995, 36, 4521.
5. Rebouillat, S.; Escoubes, M.; Gauthier, R.; Vigier, A. *J Appl Polym Sci* 1995, 58, 1305.
6. Rebouillat, S.; Donnet, J. B.; Guo, H.; Wang, T. K. *J Appl Polym Sci* 1998, 67, 487.
7. Rebouillat, S.; Donnet, J. B.; Wang, T. K. *Polymer* 1997, 38, 2245.
8. Rebouillat, S.; Peng, J. C. M.; Donnet, J. B. *Polymer* 1999, 40, 7341.
9. Rebouillat, S.; Escoubes, M.; Gauthier, R. *J Adhes Sci Technol* 1996, 10, 635.
10. Rebouillat, S. *J Mater Sci* 1998, 33, 3293.
11. Rebouillat, S.; Hearle, J. W. S. *High Performance Fibres*; Cambridge: Woodhead Publishing Limited, S., 2001, ISBN 1 85573 539 3, p 23.
12. Rebouillat, S.; Donnet, J. B.; Peng, J. C. M.; Wang, T. K., Series Eds. *Carbon Fibers*, Marcel Decker: New-York, 1998, ISBN 0-8247-0172-0.
13. Rebouillat, S.; Liksonov, D. *Comput Fluids* 2010, 39, 739.
14. Qiu, Y.; Wang Y. A Novel Approach for Measurement of Fiber-on-fiber Friction. Available at: <http://www.p2pays.org/ref/08/07122.pdf>. Accessed on September 98.
15. Mano, J. F.; Lopes, J. L.; Silva, R. A.; Brostow, W. *Polymer* 2003, 44, 4293.
16. Alwis, K. G. N. C.; Burgoyne, C. J. *Appl Compos Mater* 2006, 13, 249.
17. Peng, Y. X.; Zhu, Z. C.; Chen, G. A. *Min Sci Technol (China)* 2009, 19, 518.
18. Vargas, A. F.; Orozco, V. H.; Rault, F.; Giraud, S.; Devaud, E.; Lopez, L. L. *Compos Appl Sci Manuf* 2010, 41, 1797.
19. Hufenbach, W.; Bohm, R.; Thieme, M.; Winkler, A.; Mader, E.; Rausch, E.; Shade, M. *Mater Des* 2011, 32, 1468.
20. Varela-Rizo, H.; Weisenberger, M.; Bortz, D. R.; Martin-Gullon, I. *Compos Sci Technol* 2010, 70, 1189.
21. Błazewicz, S.; Wajler, C.; Chlopek, J. *J Biomed Mater Res* 1996, 32, 215.
22. Leech, C. M. *Int J Mech Sci* 2002, 44, ISSN 0020-7403, 621.
23. Elert, G. Available at: http://en.wikipedia.org/wiki/Harmonic_oscillator. Accessed on September 2009.
24. Treichler, J. Available at: http://en.wikipedia.org/wiki/Finite_impulse_response. Accessed on May 2010.